

# Analysis of Solid-State Transformer Enabled Hybrid Microgrid using Resilience Energy Amendment Control Algorithm

Mr. J. Vijay<sup>1\*</sup>, Dr. L.K. Hema<sup>2</sup>

Submitted: 10/11/2022

Accepted: 11/02/2023

**Abstract:** The increasing electricity demand has attracted global attention and led energy producers and marketers to develop a modified converter circuit for energy stability. In this case, a Dual Active Bridge (DAB) based DC-DC converter is implemented to attain a higher voltage conversion ratio by varying the switching function of the converter. The purpose of the current study is to create soft-switching DAB converter that decreases turn-off switching loss and delivers steady energy power flow in a DC bus system. The DAB converter adopted runs in two modes: boost and buck. The switch is closed in both phases of operation of the converter to decrease zero current loss and increase converter efficiency. The suggested circuit would draw power from the battery sources to control the output load while preserving high efficiency and reliability in power transfer. They are simple and dependable control methods based on the Resilience Energy Amendment Control (REAC) algorithm. The REAC controller has the advantage of adjusting the PWM of the DAB on the fly while maintaining a desired constant output voltage. To achieve this goal, the reference value of the input voltage is adjusted spontaneously well, fine-tuning the duty cycle, low zero constant-state error, fast response and output load and low noise sensitivity. This simulation was MATLAB 2017 b software, and the results showed the performance and reliability of the circuits. The performance of the implemented system is evaluated depends on different parameters like steady-state error (%), Total Harmonics Distortions (THD %) and efficiency (%) of the system.

**Keywords:** Dual Active Bridge (DAB), Resilience Energy Amendment Control (REAC), Steady State Error, Total Harmonics Distortions (THD), modified DC-DC converter circuit, Solid State Transformer.

## 1. Introduction

In recent years, many energy stabilizations of Renewable Energy Sources (RES) like solar, wind and fuel cell and power converter technology have been introduced. The implementation of the DAB, the backup battery system plays a significant role in transmitting power from low to high voltage in both directions. The DAB converter is used at the center of the system to stabilize the DC bus system to achieve the required voltage level and reduce design and size costs. DAP converters are used at high voltage gain to sensitize their switching devices through the transformer using a smooth switching function and auxiliary passive resonant circuits that maintain the essential voltage at the converter circuit end.

The implemented Resilience Energy Amendment Control (REAC) based soft switch techniques provide an appropriate pulse to the converter. The proposed converter

circuit improves parameters such as minimizing switching loss, higher power, and higher switching frequency and improves performance. A new isolated DAB scheme and Zero Current Switching (ZCS) transmission are implemented. This DC-DC converter, which reaches the high gain separation DAB, has additional additions to the active and passive vibration circuits. This research aims to improve the power generation of the renewable energy system and consistent power flow in DC and AC bus systems.

The adequate backgrounds are the buck and boost converters that have been suggested, depends on minimum ripple of interleaved structures for maximum power applications. Nevertheless, this maximizes the volume of the converter, reducing their power density and efficiency. Coupled inductors were used in this study. Though, this leads to hysteresis loss and ripple current loss, reducing the efficiency of the converter. In addition, leakage inductance may cause voltage spikes across switches, requiring the use of voltage clamping systems to preserve voltage stresses across the switches to minimum.

The main objective is used to convert from the fixed DC voltage and given two different constant outputs, to step up and step down the fixed voltage, to achieve High efficiency and Low noise, To Improve power quality of

<sup>1</sup>Research Scholar, Engineering and Technology – EEE, Vinayaka Mission's Research Foundation, Salem, Tamilnadu, India.

<sup>1</sup>Assistant Professor, Department of Electronics and Communication Engineering, Aarupadai Veedu Institute of Technology, Vinayaka Mission's Research Foundation, Chennai, Tamilnadu, India

<sup>2</sup>Professor, Department of Electronics and Communication Engineering, Aarupadai Veedu Institute of Technology, Vinayaka Mission's Research Foundation, Chennai, Tamilnadu, India

\* Corresponding Author Email: jvijay9902@gmail.com



voltage variation and interruptions such as high voltage. A power management system (PMS) efficiently programmed and enhanced with the DAB converter based on REAC. Lastly, the stabilized DC outage is delivered to the inverter for grid connected application.

### 3.1 Solar power generation

The basic function of Photovoltaic (PV) system is PV cell. It is connected to electricity to form a set of units of PV modules; several modules of the PV array panel are formed, and different panels are formed in series and parallel combination. The series connection is responsible for improving the system's voltage, and parallel connection improves the current flow in the system.

The influence of a series resistor on a PV model requires the usage of a recursive equation to predict output current as a function of terminal voltage for similar conditions of irradiance and p-n junction temperature. The Newton-Raphson approach converges faster and it is applicable to positive and negative currents. The PV system converts sunlight directly into electricity. The central device of photovoltaic system refers solar cell that is connected together to form panels or arrays. Power electronic converter is essential to process the electricity produced with photovoltaic devices. These converters may be utilized to manage voltage and current across a load, control power flow on grid-connected systems, and maximum power point tracking (MPPT).

Based on MPPT, the proposed Resilience Energy Amendment Control (REAC) will vary the pulse, which operations are described below.

#### 3.1.1 Resilience Energy Amendment Control (REAC)

The Resilience Energy Amendment Control (REAC) algorithm depends on exploring the relationship between output power and the voltage of a photovoltaic module. Solar panels and operating principles based on the MPP power curve behaviors are as follows: The MPPT voltage of the PV panel system is supplied with the controller by measuring the open-circuit voltage received on plate. This REAC technique assumes that the MPP voltage is constant for small fraction of the open-circuit voltage.

The control-to-output transfer function for tiny signals must be calculated in order to represent the dynamics of the SAB topology, i.e. using poles and zeroes. From the above it is clear that the duty ratio is affected by input voltage, the maximum current of inductor, the output voltage and the switching frequency. As a result of the duty ratio, the system now has state-feedback and feed forward. The capacitor voltage, which is determined by the state variable, does not include any information about the duty ratio's dependency on minor fluctuations around their steady state value. The state-space averaged model is used

at conjunction with the state-space averaged model in order to keep this information

$$V_{mpp} = K_1 * V_{oc} \quad (1)$$

In this manner, short-circuit current changes by measuring the voltage PV, the panels and provides feedback to the controller. This method: The photovoltaic panel converts the MPP current and short circuit current at straight line. The constant  $K_2$  photovoltaic energy generation based on atmospheric conditions.

$$I_{mpp} = K_2 * I_{sc} \quad (2)$$

The operation of DC-DC converter stabilized solar power generation depends on MPPT control technology will be explained. Figure 2 shows that Solar Based MPPT System.

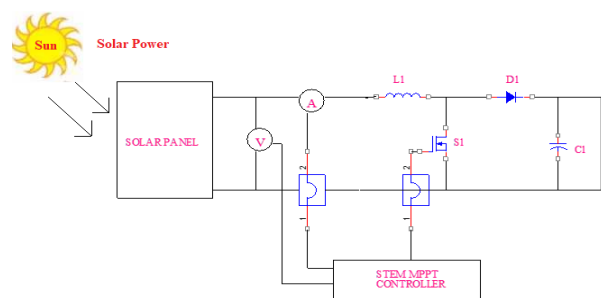


Fig. 2: Solar Based MPPT System

#### 3.1.2 Algorithm steps

**Step1:** Sense  $V_k = V_{pv}$ ,  $I_k = I_{pv}$  from the solar panel.

**Step2:** Compute  $P_k = V_k * I_k$

**Step3:** Check if  $P_k - P_{k-1} = 0$

**Step4:** If false, check if  $P_k - P_{k-1} > 0$

**Step5:** If true, check if  $V_k - V_{k-1} > 0$

1. If true increase  $V_{ref}$
2. If false decrease  $V_{ref}$

**Step 6:** If false from the fifth step, check if  $V_k - V_{k-1} > 0$

3. If true decrease  $V_{ref}$
4. If false increase  $V_{ref}$

here  $P_k$  refers energy generation of PV,  $V_{pv}$  implies solar voltage,  $I_{pv}$  is PV current,  $V_{ref}$  implies reference voltage.

### 3.2 Wind power Generation

This system contains the wind turbine rotor and Permanent magnet Synchronous Generator (PMSG), rectifier and boost converter. Wind energy converter transforms wind energy into mechanic energy, and electric generator produces electricity. Therefore, the expression of mechanical power created by wind turbine;

$$P_m = \frac{1}{2} \rho \pi R^2 V^3 C_p(\lambda, \beta) \quad (3)$$

The power coefficient (CP) of the turbine defines the power extraction capacity of wind turbine. The linear task of tip velocity ratio ( $\omega$ ) of two blades and blade pitch angle ( $\beta$ ). The theoretical value determined around 0.59, which is situated concerning 0.4 and 0.45 application. The tip Velocity refers ratio of the output of the variable blade tip, which the wind turbine rotation can specify to accelerate the linear velocity and equation (9):

$$C_p(\lambda, \beta) = 0.5(116 \frac{1}{\lambda_i} - 0.4\beta - 5) e^{-\frac{21}{\lambda_i}} \quad (4)$$

$$\frac{1}{\lambda_i} = \frac{1}{\lambda_i + 0.08\beta} - \frac{0.032}{1 + \beta^3} \quad (5)$$

Also, in this work, the angle ( $\beta$ ) is set to zero because of the assumption of constant pitch rotor. Therefore, the main feature of  $C_p$  is depends on  $u$ . The Resilience Energy Amendment Control (REAC) method seems simple because the wind speed is direct and continuous measurement provides accurate wind speed measurement. In reality, it is impossible and increases the cost of the system.

### 3.3 Fuel cell energy generation

Due to the fuel cells limitation, including low voltage and current density and instantaneous energy generation. Generally, only 0.3, 0.5 volts per load, direct methanol fuel cell is supplied.

### 3.4 Battery modeling

The best operational conditions are necessary to meet the load requirements. To provide the desired energy while the battery is sufficient, of course, are set to be enormous to see better battery charging, which is calculated as below:

$$B_{cs}(t) = B_{ds}(t - 1) + ((B_{cc}(t-1) + B_t(t - 1)) \cdot C_{bat} \quad (6)$$

Where  $B_{CS}(t)$  = charging time of the battery

$B_{ds}(t - 1)$  = discharging time of battery t-1,

$B_{cc}(t - 1)$  = amount of charge stored in the battery

$B_t(t-1)$  = total amount of energy delivered at the timet

$C_{bat}$  = charging efficiency of the battery.

Depending on load requirements and level of energy supplied with RES generation level, the battery state of charge (SOC) is calculated using the formula below:

i) During charging mode,

$$SOC(t) = SOC(t - 1) + \frac{B_{bat(t)} B_{char}}{P_N} \quad (7)$$

ii) During discharging mode,

$$SOC(t) = SOC(t - 1) + \frac{B_{bat(t)} B_{dis}}{P_N} \cdot 100 \quad (8)$$

Based on RES power generation, the SOC state of battery mode is regulated by the proposed Resilience Energy Amendment Control (REAC) controller.

### 3.5 Dual active bridge converters

The implemented proposed DAB converter is represented in figure 3. A possible alternative for realizing DAB converter topology is the back-to-back high-power two-way DC-DC converter with any single-phase voltage. For each of these arrangements, the series inductor is controlled to regulate the DAB power flow converter. The flow between each side is connected by changing amplitude and phase angle variation of the AC output voltages.

Solid State Transformer (SST) based on high frequency power electronics converter is gaining a lot of attention as a key component of developing smart distribution systems with many features like reactive power control, voltage regulation, power quality and an efficient interface for distributed generation and storage. Compared with standard bulky and heavy low frequency transformer, the distribution transformers size and weight may be greatly decreased by adopting high frequency SST. Furthermore, state-of-art solid-state electronics, like new generation devices, SST may reach high efficiency comparable to traditional line frequency transformer.

The switching devices are more difficult to select because they do not require any mathematical analysis and must be chosen using best judgment. MOSFET resistance, peak voltage or current ratings, and the stresses they must withstand are all factors that contribute to switching devices. It contains values for peak direct and indirect current flow with the chosen energy transfer inductor, which limits both the conductive functionality of the chosen devices and the opposition that individuals must have to reduce the loss.

The primary side of converter transforms the incoming DC voltage into AC voltage that flows to transformer. A secondary side converter rectifies and generates a voltage (DC) which is then supplied to the load. Both sources in both directions can use a DC-DC converter if both load and source are DC. The bi-directional DABDC-DC Converter is most commonly used because it can make current flow in both directions (forward and reverse direction).

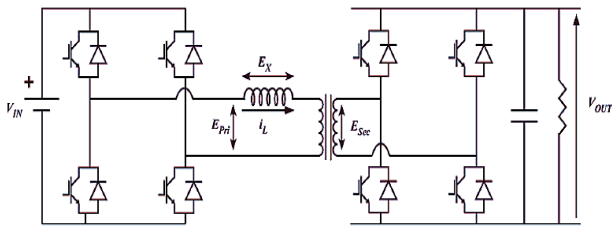


**Fig. 3** Circuit diagram for proposed Dual Active Bridge

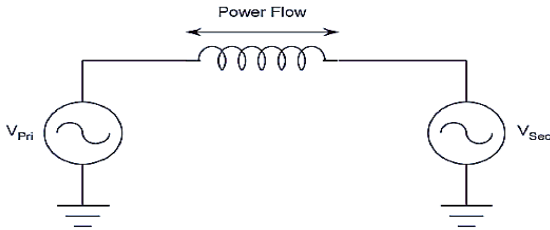


**Fig. 4:** Power flow of grid-connected system and phasor analysis of the interconnected transmission system

The structure is similar to the series inductor connected to the grid, as illustrated in Figure 4. Thus, controlling the active and reactive power for an overflow accepted principles can connect the two AC sources is applied to the dual inverter topologies.

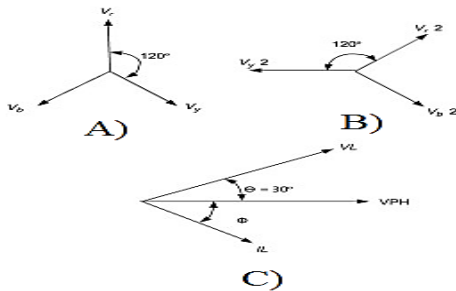


**Fig. 4 (A):**  $V_{pri}$  power flow  $Q$ , (B) both input power  $Q$ , and (C)  $V_{sec}$  Power flow  $Q$

Figure 4(A) represents the energy power flow between the two grids connected system, and the current flow based voltage variation is expressed below;

$$I \angle \theta = \frac{V_{pri} \angle \delta - V_{sec} \angle 0}{j\omega L} \quad (9)$$

where  $\delta$  is the relative amount of angle among two voltage sources;  $V_{pri}$  and  $V_{sec}$  source voltage amplitude is two, and  $\omega$  refers fundamental frequency. Multiplying the  $V_{sec}$  by the real part and reactive power given by equation (16) into auxiliary source is:

$$S_{sec} = P_{sec} + jQ_{sec} = V_{sec} \left\{ \frac{V_{pri} \angle \delta - V_{sec}}{j\omega L} \right\} \quad (10)$$

$$P_{sec} = \frac{V_{pri} V_{sec} \sin \delta}{\omega L} \text{ and } Q_{sec} = \frac{V_{pri} V_{sec} \cos \delta - V_{sec}^2}{\omega L} \quad (11)$$

The actual power shown in (16) is mainly propagated by the magnitude of the phase angle between source voltage determined by the angle, and the power transfer is mostly determined by the magnitude of voltage variance among two.

The implemented Resilience Energy Amendment Control (REAC) method was adopted to block each transformer in a two-way system (square wave) and change the converter's square wave output compared to controlled power transmission. However, the output waveform of each converter is now filled, but it raises a low-frequency uniform frequency sound based on the transmitting power and square wave synchronization. Therefore, the actual transmission power in each sense of the harmonics must be abbreviated to determine the total power transmission between the two bridges. The square wave output equation (16), which is accomplished by determining each harmonic component individually and combining their contributions, can be applied to each Fourier transformer using the harmonic components:

$$P = \frac{1}{1} \sum_{n=0}^{\infty} \left[ \frac{4V_p}{[2n+1]} \times \frac{4V_s}{[2n+1]} \times \frac{\sin[2n+1]\delta}{[2n+1]\omega_s L} \right] \quad (12)$$

For a single-phase system, each converter or three-phase switch uses any simple two-stage square wave switch, where the two-phase legs 180 of the square wave conversion of the phase switch are controlled by the two-phase branch of each converter. The potential advantage of the second method is the phase and purpose. Each converter's output can vary independently, but the resulting waveform change is a more complex analysis and interpretation. The only possible option for a three-phase system with two converters is to convert the three-phase arms of each 120 by creating a well-known six-stage modulation output.

### 3.6 Voltage source inverter

The implemented Resilience Energy Amendment Control (REAC) control scheme for Voltage Source Inverter (VSI) depends on active power/frequency and reactive power/voltage drop in the traditional micro grid, as well as frequency and phase detection with a phase-locked loop (PLL). The PLL determines the frequency and establishes the phase reference for the inverter using the voltage components of and. The quantity supplied to a phase adjuster was determined together with the intended phase of the inverter output.

The voltage regulator calculates and modifies the desired voltage amplitude of the inverter. Single phase VSIs are utilized for less power applications while three phase VSIs are utilized for medium to high power applications. The key purpose of these topologies is to deliver a three-phase voltage source with control over the amplitude, phase and

frequency of voltages. An uninterruptible power supplies to generate alternating current voltage magnitudes and controllable frequency via several pulse width modulations (PWM) approaches. Finally, the PWM generator takes the amplitude and phase of the desired voltage creates a PWM output signal.

The power flow of transmission line at d-q axis control point depends on the exact measurement of the actual and reactive forces. For the response speed inverter control system, the traditional definition of active and reactive power cannot meet this requirement over an average period. Instantaneous power theory provides powerful tool for real-time control of power systems. In a balanced three-phase power system, there is no zero or negative sequence component. The three-phase voltage may be expressed as below,

$$V(x) = \begin{cases} V_r = V \cos(\omega t) \\ V_y = V \cos(\omega t - 120) \\ V_b = V \cos(\omega t + 120) \end{cases} \quad (13)$$

The current flow in the circuit is written as;

$$I(x) = \begin{cases} I_r = I \cos(\omega t - \theta) \\ I_y = I \cos(\omega t - \theta - 120) \\ I_b = I \cos(\omega t - \theta + 120) \end{cases} \quad (14)$$

where;

V= peak voltage

I =peak value of the currents.

The voltage & current matrix expression are described below;

$$\bar{v} = \begin{bmatrix} V_a \\ V_b \\ V_c \end{bmatrix}, \bar{i} = \begin{bmatrix} i_a \\ i_b \\ i_c \end{bmatrix} \quad (15)$$

The switching behavior of the proposed REAC controller is represented in table 1.

**Table 1:** Inverter Switching Sequence

Switching Sequence						Load Line
S <sub>1</sub>	S <sub>2</sub>	S <sub>3</sub>	S <sub>4</sub>	S <sub>5</sub>	S <sub>6</sub>	Voltage
1	0	0	0	0	1	+V <sub>dc</sub> /2
1	1	0	0	0	0	+V <sub>dc</sub> /2
0	1	1	0	0	0	0
0	0	1	1	0	0	-V <sub>dc</sub> /2
0	0	0	1	1	0	-V <sub>dc</sub> /2
0	0	0	0	1	1	0

### 3.7 Resilience Energy Amendment Control (REAC)

The transmission of electricity from renewable energy sources to multiple power sources must properly address

stability and power quality issues. Therefore, the operating voltage of the power of this system is designed to prevent the rescheduling, and greater this point puts the power to function normally. The PMS is efficiently programmed and enhanced with DAB converter based on REAC. At last, the stabilized DC outage is delivered to inverter for grid-connected application.

#### 3.7.1 REAC Algorithm Steps

**Step1:** Initialization of devices.

**Step2:** At first, Source power is ON condition.

**Step3:** Devices are executed by DC power

**Step4:** REAC controller is scheduled to monitor source power generation like (solar, wind and fuel cell) as well as grid power.

**Step 5:** If hybrid power generation is different under threshold, the REAC controls the PWM control signal with DAB converter until the condition; if false, check if  $P_k - P_{k-1} > 0$  (or) If true, check if  $V_k - V_{k-1} > 0$  is fulfilled.

**Step 6:** In REAC controller, the stored energy is continuously related to preset levels. If the power supply is stable, the battery is in a charging condition; otherwise it will discharge and compensate the load power.

**Step 7:** The stabilized power is delivered with inverter.

Here, V<sub>s</sub>=source voltage, P<sub>i</sub>=input power, V<sub>out</sub>=output voltage, C<sub>p</sub>=control power

**Step 8:** Compute d and q-axis components of grid system voltage

$$V_d = L \frac{d i_d}{dt} - \omega L i_q + V_{gd} \quad (16)$$

$$V_q = L \frac{d i_q}{dt} - \omega L i_d + V_{gq} \quad (17)$$

**Step 9:** Comparison between terminal (V<sub>a</sub>, V<sub>b</sub>, V<sub>c</sub>) voltages measured depends on control together with reference voltage V<sub>dref</sub>, and V<sub>qref</sub>.

**Step 10:** The control of REAC reference optimized voltages are calculated as several load as well as source voltage.

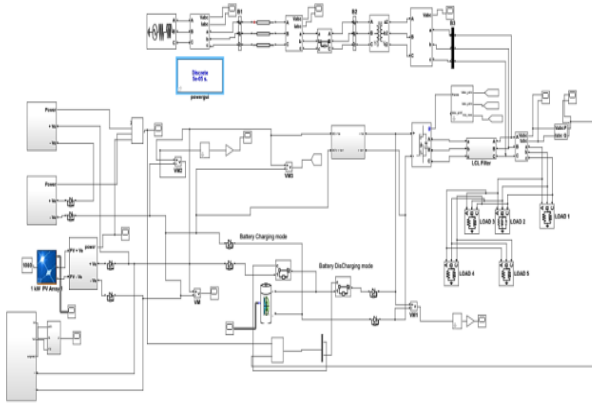
**Step 11:** The average value function as well as output of filter depend on the actual power consumption of the positive line.

**Step 12:** Terminate.

## 4. Result and Discussion

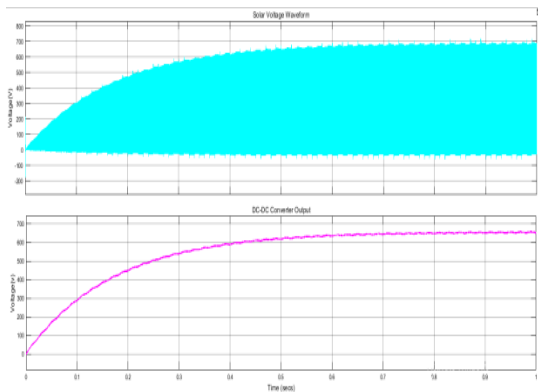
The present modeling method was developed in Matlab-based toolbox. The OBD converter based on the proposed REAC technique is analyzed under several operating

conditions. The new proposed REAC model is executed atmatlab environment. The REMS creates the system power source with a dissimilar way of power generation. The inadequate power sources will be controlledthrough a converterthat enhances the voltage on source side. The system power control is required to regulate the power using the REAC controller.



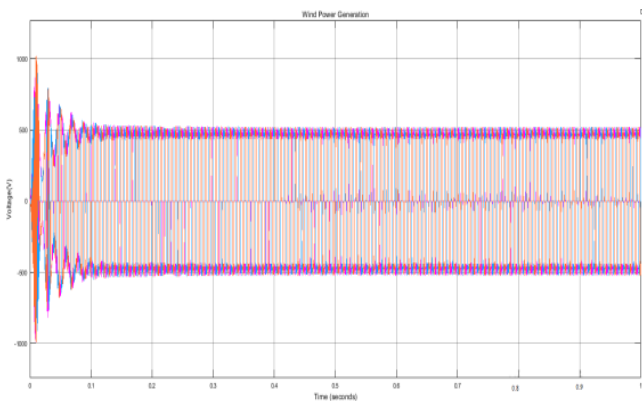
**Fig. 5** Proposed Simulink Model

Figure 5 represents the Simulink model grid, and the combined hybrid system comprises fuel cell, wind, solar, and battery system. The proposed method is used for hybrid power synchronization output, which is given below.



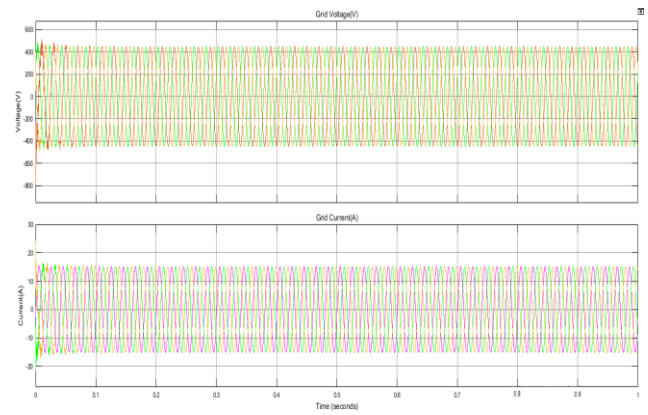
**Fig. 6 (i)** Solar output power

The power output from the Solar power is shown in Figure 6 (i) for the generated voltage  $V = 600$  times at the time duration 1second.



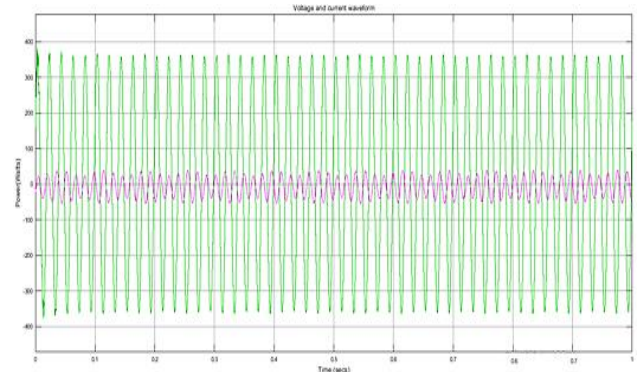
**Fig. 6 (ii)** wind power

The energy output for the maximum power wind sample with the obtained voltage: 500 V using time  $t = 1$  second is shown on figure 6 (ii).



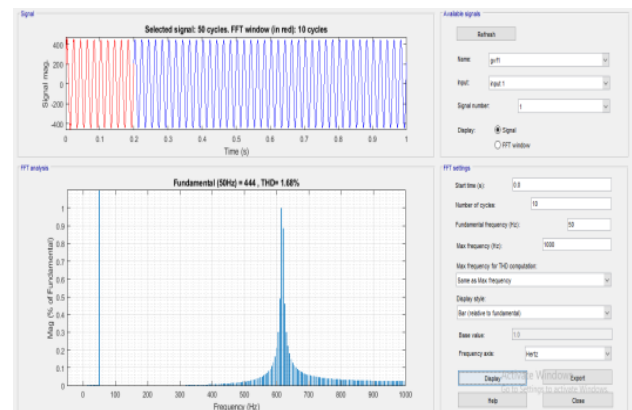
**Fig. 6 (iii)** Grid Power Waveform

The power of the optimal grid voltage and the current grid is shown in Figure 6 (iii). The y-axis represents the phase supply voltage 440v, and the x-axis represents the time  $T = 1$  seconds. According to the load, the current display of the waveform is displayed on y-axis = 15A, and x-axis represents  $T = 1$  second.



**Fig. 6(iv)** Load current and Voltage waveform

Figure 6 (iv) represents load voltage and current waveforms which are the differential time periods relating to everyone.



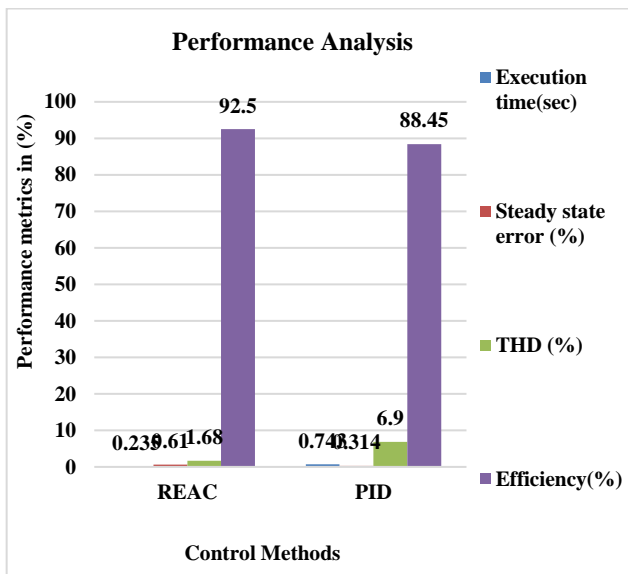
**Fig. 6(v)** THD analysis

Figure 6 (v) portrays harmonics distortions analysis of the system. Based on the load voltage-based THD analysis, the proposed REAC is generating a 1.68% THD Ratio.

**Table 2 (a):** Comparative analysis of proposed system

Parameters	PID	REAC
Execution time(sec)	0.743	0.235
Steady-state error (%)	0.61	0.314
THD (%)	6.5	1.68
Efficiency (%)	88.45	92.5

Table 2 (a) shows that Comparative analysis of proposed system. From the comparative analysis of all those parameters, it is confirmed that the proposed Resilience Energy Amendment Control (REAC) control strategy produces an efficient result.



**Fig. 6(vi)** Performance analysis

Figure 6 (vi) shows the comparative analysis of proposed system: According to analysis, it is understood that proposed Resilience Energy Amendment Control (REAC) creates a better outcome related to the conventional methods.

**Table 2 (b)** Performance of the power factors for several Loads

Controller	Power Factor (P.F)	Load (W)
REAC	0.9989	0
	0.9972	200

0.9970	400
0.9968	600
0.9962	800
0.9958	1000

Table 2 (b) defines performance of power factor variation for inverter output power under load changing conditions.

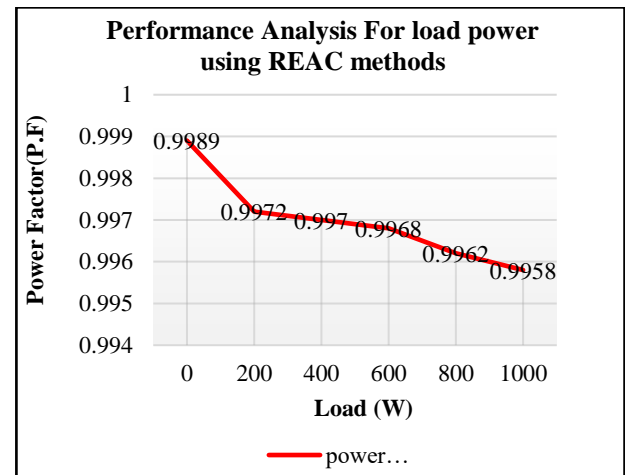


**Fig. 6 (vii)** Performance Power Factor graphs under load varying conditions

Figure 6 (vii) portrays performance of power factor under load varying conditions. The Resilience Energy Amendment Control (REAC) controller will create efficient outcomes under variable load conditions (0-1000).

**Efficiency** **Formula:** Efficiency =  $\frac{\text{Maximum Possible output}}{\text{Actual Input}} \times 100\%$  (18)

$$\text{Actual input power} = 7000 \text{ W}$$

$$\text{Maximum possible output} = 440(\text{V}) \times 15.5 (\text{A}) = 6820 \text{ W}$$

$$= \frac{6820}{7000} \times 100\%$$

$$= 0.985 \times 100\%$$

$$\text{Efficiency} = 98.5\%$$

**Power Factor:** 98.5

$$\text{Power Factor} = \frac{\text{True Power}}{\text{Apparent Power}}$$

$$= \frac{998}{1000}$$

$$\text{PF} = 0.998$$

## 5. Conclusion

A newly implemented Dual Active Bridge (DAB) converter topology has been presented in this work. Design

and theoretical analysis of a DAB converter with new soft-switching techniques will improve the performance of proposed system. This converter works in forwarding power transmission (boost) and power transmission (buck) mode based on the reverse of switching action of proposed REAC controller. The main MOSFET is turned off, and the ZCS is retrieved, while the converter is operated in boost and buck modes. The smooth transition from input to output power is through the Resilience Energy Amendment Control (REAC) independent duty rotation control. Also, it uses resonance triggers, which make the scale compact and easy to control. The converter may be operated in boost operation and buck mode. The static-level analysis of proposed converter analyzes the performance under different load conditions, given the above results. The performance of the proposed Resilience Energy Amendment Control (REAC) control techniques are examined with dissimilar parameters as steady-state error 0.326 % THD 1.68 %, and the efficiency of the Resilience Energy Amendment Control (REAC) of the system is beyond comparison as it provides phenomenal results.

## References

- [1] Y. Xiao, Z. Zhang, K. T. Manes and M. A. E. Andersen, "A Universal Power Flow Model for Dual Active Bridge-Based Converters With Phase Shift Modulation," in *IEEE Transactions on Power Electronics*, vol. 36, no. 6, pp. 6480-6500, 2021.
- [2] S. Pugliese, G. Buticchi, R. A. Mastromauro, M. Andresen, M. Liserre and S. Stasi, "Soft-Start Procedure for a Three-Stage Smart Transformer Based on Dual-Active Bridge and Cascaded H-Bridge Converters," in *IEEE Transactions on Power Electronics*, vol. 35, no. 10, pp. 11039-11052, 2020
- [3] T. Uchida, Y. Ishizuka, D. Yamashita, T. Hirose and K. Ura, "A Control Method of Dual Active Bridge DC-DC Converters Maintaining Soft-Switching at Different Voltage Ratio," *2020 IEEE Applied Power Electronics Conference and Exposition (APEC)*, pp. 3364-3370, 2020.
- [4] Y. Guan, Y. Xie, Y. Wang, Y. Liang and X. Wang, "An Active Damping Strategy for Input Impedance of Bidirectional Dual Active Bridge DC-DC Converter: Modeling, Shaping, Design, and Experiment," in *IEEE Transactions on Industrial Electronics*, vol. 68, no. 2, pp. 1263-1274, 2021.
- [5] A. N. S. J. T.G. and V. John, "Minimum Leakage Inductance for Soft-switching of Dual-Active Half-Bridge DC-DC Converter," *2020 IEEE International Conference on Power Electronics, Drives and Energy Systems (PEDES)*, pp. 1-6, 2020.
- [6] D. Sha, J. Zhang and K. Liu, "Leakage Inductor Current Peak Optimization for Dual-Transformer Current-Fed Dual Active Bridge DC-DC Converter With Wide Input and Output Voltage Range," in *IEEE Transactions on Power Electronics*, vol. 35, no. 6, pp. 6012-6024, 2020.
- [7] Y. Wang, Y. Zhu and H. Wen, "PSO-based Current Stress Optimization for Three-Level Dual Active Bridge DC-DC Converters," *2020 Chinese Automation Congress (CAC)*, pp. 4283-4287, 2020.
- [8] M.A. Awal, M.R. Bipu, O.A. Montes, H. Feng, I. Husain, W. Yu, S. Lukic. "Capacitor Voltage Balancing for Neutral Point Clamped Dual Active Bridge Converters," in *IEEE Transactions on Power Electronics*, vol. 35, no. 10, pp. 11267-11276, 2020
- [9] A. K. Bhattacharjee and I. Batarseh, "An Interleaved Boost and Dual Active Bridge-Based Single-Stage Three-Port DC-DC-AC Converter With Sine PWM Modulation," in *IEEE Transactions on Industrial Electronics*, vol. 68, no. 6, pp. 4790-4800, 2021.
- [10] J. Deng and H. Wang, "A Hybrid-Bridge and Hybrid Modulation-Based Dual-Active-Bridge Converter Adapted to Wide Voltage Range," in *IEEE Journal of Emerging and Selected Topics in Power Electronics*, vol. 9, no. 1, pp. 910-920, 2021.
- [11] S. S. Shah and S. Bhattacharya, "A Simple Unified Model for Generic Operation of Dual Active Bridge Converter," in *IEEE Transactions on Industrial Electronics*, vol. 66, no. 5, pp. 3486-3495, 2019.
- [12] S. S. Shah, V. M. Iyer and S. Bhattacharya, "Exact Solution of ZVS Boundaries and AC-Port Currents in Dual Active Bridge Type DC-DC Converters," in *IEEE Transactions on Power Electronics*, vol. 34, no. 6, pp. 5043-5047, 2019.
- [13] Z. Guo and D. Sha, "Dual-Active-Bridge Converter With Parallel-Connected Full Bridges in Low-Voltage Side for ZVS by Using Auxiliary Coupling Inductor," in *IEEE Transactions on Industrial Electronics*, vol. 66, no. 9, pp. 6856-6866, 2019.
- [14] H. Shi, K. Sun, H. Wu and Y. Li, "A Unified State-Space Modeling Method for a Phase-Shift Controlled Bidirectional Dual-Active Half-Bridge Converter," in *IEEE Transactions on Power Electronics*, vol. 35, no. 3, pp. 3254-3265, 2020.
- [15] B. Rahrovi, R. T. Mehrjardi and M. Ehsani, "On the Analysis and Design of High-Frequency Transformers for Dual and Triple Active Bridge Converters in More Electric Aircraft," *2021 IEEE Texas Power and Energy Conference (TPEC)*, pp. 1-6, 2021.

- [16] K. Sumiya, Y. Naito, J. Xu, N. Shimosato and Y. Sato, "An Advanced Commutation Method for Bidirectional Isolated Three-Phase AC/DC Dual-Active-Bridge Converter Based on Matrix Converter," *2020 IEEE Energy Conversion Congress and Exposition (ECCE)*, pp. 4158-4164, 2020.
- [17] F. Liu, X. Sun, J. Feng, J. Wu and X. Li, "The improved dual active bridge converter with a modified phase shift and variable frequency control," *2018 IEEE Applied Power Electronics Conference and Exposition (APEC)*, pp. 814-819, 2018.
- [18] S. Bal, D. B. Yelaverthi, A. K. Rathore and D. Srinivasan, "Improved Modulation Strategy Using Dual Phase Shift Modulation for Active Commutated Current-Fed Dual Active Bridge," in *IEEE Transactions on Power Electronics*, vol. 33, no. 9, pp. 7359-7375, 2018.
- [19] X. Liu, Z.Q. Zhu, D.A. Stone, M.P. Foster, W.Q. Chu, I. Urquhart, J. Greenough, "Novel Dual-Phase-Shift Control With Bidirectional Inner Phase Shifts for a Dual-Active-Bridge Converter Having Low Surge Current and Stable Power Control," in *IEEE Transactions on Power Electronics*, vol. 32, no. 5, pp. 4095-4106, 2017
- [20] Y. Shi, R. Li, Y. Xue and H. Li, "Optimized Operation of Current-Fed Dual Active Bridge DC-DC Converter for PV Applications," in *IEEE Transactions on Industrial Electronics*, vol. 62, no. 11, pp. 6986-6995, 2015.
- [21] H. Wu, L. Chen and Y. Xing, "Secondary-Side Phase-Shift-Controlled Dual-Transformer-Based Asymmetrical Dual-Bridge Converter With Wide Voltage Gain," in *IEEE Transactions on Power Electronics*, vol. 30, no. 10, pp. 5381-5392, 2015.
- [22] L. Xue, Z. Shen, D. Boroyevich, P. Mattavelli and D. Diaz, "Dual Active Bridge-Based Battery Charger for Plug-in Hybrid Electric Vehicle With Charging Current Containing Low Frequency Ripple," in *IEEE Transactions on Power Electronics*, vol. 30, no. 12, pp. 7299-7307, 2015.
- [23] Z. Zhang, O. C. Thomsen and M. A. E. Andersen, "Soft-Switched Dual-Input DC-DC Converter Combining a Boost-Half-Bridge Cell and a Voltage-Fed Full-Bridge Cell," in *IEEE Transactions on Power Electronics*, vol. 28, no. 11, pp. 4897-4902, 2013.
- [24] B. Zhao, Q. Song, W. Liu, G. Liu and Y. Zhao, "Universal High-Frequency-Link Characterization and Practical Fundamental-Optimal Strategy for Dual-Active-Bridge DC-DC Converter Under PWM Plus Phase-Shift Control," in *IEEE Transactions on Power Electronics*, vol. 30, no. 12, pp. 6488-6494, 2015.
- [25] M. Rolak and M. Malinowski, "Dual Active Bridge for Energy Storage System in Small Wind Turbine," *IEEE Africon 11*, pp. 1-5, 2011.